Evaluating the size and extent of paleolakes in central Tibetduring the late Pleistocene

Citation for published version:
Shi, X, Furlong, K, Kirby, E, Meng, K, Marrero, S, Gosse, J, Wang, E & Phillips, FM 2017, 'Evaluating the size and extent of paleolakes in central Tibetduring the late Pleistocene', Geophysical Research Letters, vol. 44, no. 11, pp. 5476–5485. https://doi.org/10.1002/2017GL072686

Digital Object Identifier (DOI):
10.1002/2017GL072686

Published In:
Geophysical Research Letters

AGU PUBLICATIONS

Geophysical Research Letters

RESEARCH LETTER
10.1002/2017GL072686

Key Points:
- Estimates of flexural rebound test the hypothesis of extensive ancient lake in Tibet
- Shorelines ~50-100 m above present-day Siling Co dated to 110-190 ka
- MIS 5e shoreline positions at Siling Co preclude continuous, deep lake across central Tibet

Supporting Information:
- Supporting Information S1

Correspondence to:
X. Shi and K. Meng,
xshi@ntu.edu.sg;
michael.meng@mail.iggcas.ac.cn

Citation:
Shi, X., K. P. Furlong, E. Kirby, K. Meng, S. Marrero, J. Gosse, E. Wang, and F. Phillips (2017), Evaluating the size and extent of paleolakes in central Tibet during the late Pleistocene, *Geophys. Res. Lett.*, *44*, 5476–5485, doi:10.1002/2017GL072686.

Received 30 JAN 2017
Accepted 30 MAY 2017
Accepted article online 31 MAY 2017
Published online 12 JUN 2017

Evaluating the size and extent of paleolakes in central Tibet during the late Pleistocene

Xuhua Shi[1], Kevin P. Furlong[2], Eric Kirby[3], Kai Meng[4], Shasta Marrero[5], John Gosse[6], Erchie Wang[4], and Fred Phillips[7]

[1]Earth Observatory of Singapore, Nanyang Technological University, Singapore, [2]Department of Geosciences, Pennsylvania State University, University Park, Pennsylvania, USA, [3]College of Earth, Ocean, and Atmospheric Sciences, Oregon State University, Corvallis, Oregon, USA, [4]Institute of Geology and Geophysics, Chinese Academy of Sciences, Beijing, China, [5]School of Geosciences, University of Edinburgh, Edinburgh, UK, [6]Department of Earth Sciences, Dalhousie University, Halifax, Nova Scotia, Canada, [7]Department of Earth and Environmental Science, New Mexico Tech, Socorro, New Mexico, USA

Abstract Subhorizontal lake shorelines allow a geodynamic test of the size and extent of a hypothesized paleolake in central Tibet, the East Qiangtang Lake (EQL), during the last interglacial period (marine isotope stage (MIS) 5e). Reconstructions based on relict lake deposits suggest that the EQL would have been ~400 m deep and over ~66,000 km^2. Models of flexural rebound driven by lake recession predict that shorelines near the EQL center, at the present-day location of Siling Co, would have rebounded 60–90 m above their initial elevation. New ^{36}Cl chronology of the highest relict shorelines around Siling Co indicates that they reflect lake levels between 110 and 190 ka. These shorelines, however, are presently >300 m below their predicted elevations, implying a substantially smaller water load. Our results reveal that the expansion of Tibetan lakes during MIS 5e was relatively limited. Instead, individual lakes were supplied by river networks, much as they are today.

1. Introduction

The internally drained, high elevation regions of the central Tibetan Plateau retain hundreds of saline lakes [*Zhang et al.*, 2014], the basins of which are decorated by flights of relict shorelines that attest to more extensive lake systems in the recent geological past [*Avouac et al.*, 1996; *Gasse et al.*, 1991]. In recent years, a wealth of new chronologies from paleoshoreline deposits reveals that most of these lakes experienced highstand conditions in the early part of the Holocene [*Hudson et al.*, 2015; *Rades et al.*, 2015; *Shi et al.*, 2015] possibly in response to increased monsoonal precipitation [*Hudson and Quade*, 2013]. The Holocene highstand shorelines lie between 50 and 100 m above present lake levels [*Hudson et al.*, 2015; *Rades et al.*, 2015; *Shi et al.*, 2015], although in some hydrologically isolated basins in western Tibet, Holocene shorelines can be found up to ~250 m above modern lakes [e.g., *Avouac et al.*, 1996].

In contrast, remnants of paleoshoreline features and lacustrine deposits have been found at relatively high elevations around Nam Co, a large lake situated along the southeastern margin of the internally drained region of Tibet (Figure 1). The height of these deposits relative to water divides has led to the hypothesis that a single great lake once occupied the interior of the plateau [e.g., *Shao et al.*, 2013; *Zhu et al.*, 2004]. This lake system, referred to as the East Qiangtang Lake (EQL), is inferred to have reached a shoreline elevation of ~4860 m, implying a surface area exceeding 66,000 km^2 and water depths >300–400 m in the central basins (Figures 1 and S1 in the supporting information). Although chronologic control on these lake deposits is sparse, uranium-series dating of carbonate-rich material suggests deposition between ~40 ka and ~120 ka [*Shao et al.*, 2013; *Zhu et al.*, 2004].

The spatial extent of shorelines and deposits associated with the hypothesized EQL is not established. Lacustrine deposits observed at elevations near the inferred lake margin (~4860 m) are found only in close proximity to the modern basin of Nam Co (locations T and G, Figure 1). Therefore, correlation to ancient lacustrine deposits in other lake basins throughout Tibet is largely inferential [*Shao et al.*, 2013]. Although reconnaissance studies suggest that pre-Holocene shoreline features and deposits exist in other basins [*Kong et al.*, 2011], it remains unknown whether these shorelines represent a single EQL. Moreover, previous attempts to reconstruct the extent of lake systems at the ~4860 m level did not consider the possibility that lithospheric

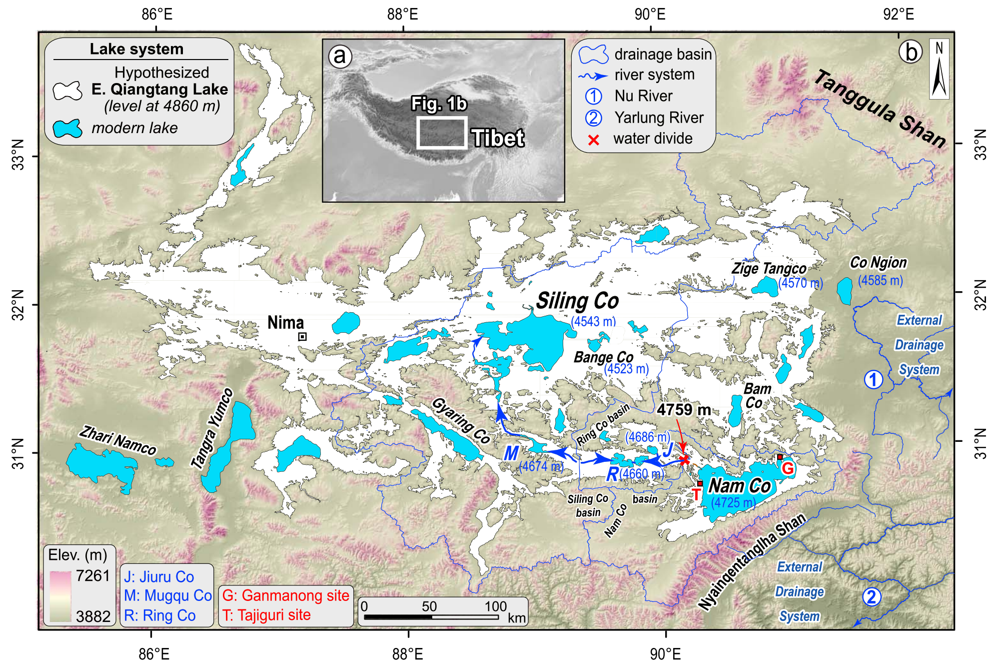

Figure 1. Geomorphic setting of the study area. (a) The map shows the location of our study region in Tibet, (b) The map showing the proposed lake extents of the East Qiangtang lake (EQL, white polygon) at ~116 ka [*Zhu et al*., 2004] and of the modern lakes (blue polygon) [*Zhang et al*., 2011b]. The red cross marks the lowest positions of water divides. T and G show locations of lacustrine sites previously found and used to define the EQL. Bracketed blue numbers show modern lake levels from Google Earth or *Zhang et al*. [2011b].

flexure associated with changes in water load may have warped shorelines away from their original horizontal [e.g., *Bills et al*., 1994a], complicating direct comparison of shorelines based on elevation alone.

To test the hypothesis of a formerly extensive lake similar to the EQL, we conducted analyses of deflection and rebound associated with loading and removal of water in the EQL basin. We compare the predicted elevation distribution of shorelines in the present day to new observations of shoreline height around Siling Co, near the center of the EQL basin (Figure 1). Because previous work had not identified these highest shorelines near Siling Co, we undertook direct dating of several well-preserved beach platforms and deposits using depth profiles of cosmogenic ^{36}Cl concentrations in beach gravels. Collectively, these data allow us to place bounds on the height of the lake level around Siling Co during marine isotope stage (MIS) 6 to 5e and provide a direct test of the hypothesis of a single continuous paleolake on the Tibetan Plateau.

2. Background

Two primary observations led to the proposition of a single expansive EQL [*Zhu et al*., 2002, 2004]. First, stratified lacustrine deposits with a U-Th age of 115.9 ± 12.1 ka from $CaCO_3$ in clay and silt [*Zhu et al*., 2004] at the Tajiguri and Ganmanong sites (labeled as “G” and “T” in Figure 1, respectively) above Nam Co are found at 4857 m in elevation (based on a leveling survey), ~150 m above the 2009 lake level [*Zhang et al*., 2011a]. Comparably high shorelines are also found in lake basins near Nam Co [*Zhao et al*., 2011; *Zhu et al*., 2002]. Second, the low position of a water divide (~100 m lower than the highest lacustrine deposits) located west of the Nam Co basin would potentially provide a connection between the Nam Co and the Siling Co basins (Figure 1). However, there have been few tests of this hypothesis, and paleoshorelines associated with the EQL previously have not been evaluated for this purpose.

The modern Siling Co sits in a broad depression that would have been near the center of the hypothesized EQL (Figure 1). Within the Siling Co basin, Holocene shorelines are recognized up to 50 m above the 2010 lake level (4543 m) [*Meng et al*., 2012a; *Shi et al*., 2014, 2015]. The highest of these, referred to as the Lingtong shoreline, sits at 4594 m (Figure 1) and represents a period of time from ~6–4 ka when Siling Co was at its

Holocene highstand [*Shi et al*., 2015]. Remnants of even higher shorelines have been observed above this level, ranging up to ~4640 m in elevation [*Li et al*., 2009; *Meng et al*., 2012b]. However, their age and significance were previously unknown. In this study, we evaluate the age of these relict shorelines around Siling Co to test whether they are consistent with the EQL hypothesis.

3. Methods

Our approach combines modeling lithospheric flexure in response to the loading and unloading of a lake, the same size of the EQL, with surveying and dating of the highest relict shorelines around Siling Co. We model the predicted elevations of EQL highstand shorelines using a forward elastic flexural model that approximates the response of a lithosphere with a uniform elastic thickness (T_e) ranging from 20 to 30 km, values that have been previously determined for the Nam Co/Siling Co region [*Jordan and Watts*, 2005; *Shi et al*., 2015] (see details in the supporting information [*Brotchie and Silvester*, 1969; *Nakiboglu and Lambeck*, 1983; *Watts*, 2001]). We anchor the lake level to the elevation at the Ganmanong site (G in Figures 1 and 2), where lacustrine sediments of ~116 ka in age are present at 4860 m [*Zhu et al*., 2004], and estimate the total water volume that would have existed in the absence of any surface deflection (Figure S1). We then calculate the deflection (or rebound) of the crust that would have been induced by this EQL water load (or its removal), recalculate the water volume, and repeat the deflection calculation. We repeat this several times until we reach a constant result. This iterative approach (see supporting information) enables us to reconstruct the EQL lake level and volume at MIS 5e, relative to the Ganmanong site.

In the Siling Co basin, we mapped relict shoreline features, including wave-cut scarps, beach ridges and platforms, and associated lacustrine deposits above the Holocene Lingtong highstand from high-resolution (0.5 m) satellite imagery and detailed field investigation. We selected the highest beach deposits with the greatest degree of preservation for surveying in the field by differential GPS [*Meng et al*., 2012a]. For three of the best preserved of these beach complexes, including the highest shoreline features, we quantified the time since abandonment of the depositional platforms by evaluating the concentration of cosmogenic ^{36}Cl in depth profiles [*Marrero et al*., 2016a, 2016b]. We selected both limestone (CRN1 and CRN5) and feldspar (CRN3) target materials to minimize effects of thermal neutron production (Figures 3 and S2). Bulk densities of the samples were determined in the field by dividing the masses of single chunks of samples by their volumes. We weighed the samples using a hanging scale with a precision of 0.01 kg. We measured their volumes in a graduated cylinder with a precision of 0.01 liter (see detailed description in the supporting information) [*Blake and Hartge*, 1986]. The ^{36}Cl samples were chemically prepared at the New Mexico Institute of Mining and Technology and the Dalhousie University, and the isotope ratios were measured at Purdue Rare Isotope Measurement Laboratory. Details of the field sampling, laboratory, and analytical protocols are described in the supporting information [*Anderson et al*., 1996; *Aruscavage and Campbell*, 1983; *Aumer*, 2010; *Dep et al*., 1994; *Desilets et al*., 2006; *Dunne et al*., 1999; *Elmore and Phillips*, 1987; *Elsheimer*, 1987; *Gosse and Phillips*, 2001; *Lifton et al*., 2014; *Marrero*, 2009, 2012; *Muzikar et al*., 2003; *Phillips et al*., 2003; *Schimmelpfennig et al*., 2009; *Stone et al*., 1996; *Wei et al*., 2002; *Yang et al*., 2008].

4. Results

4.1. Prediction of the EQL Size and Shoreline Elevations

Our results show that the depth of the EQL water load between the inferred elevation of the EQL highstand (4860 m) and present lake levels would have reached up to 400 m (Figure S1). Removal of such a load from the lithosphere would induce significant flexural rebound and doming of any horizontal datum (Figure 2). Thus, for elastic thicknesses of 20–30 km [*Jordan and Watts*, 2005; *Shi et al*., 2015], we expect shorelines developed near the center of the EQL to have been deflected upward by ~60–90 m (Figures 2a and 2b). The model results also indicate that the elevation of the surface of the EQL, anchored to deposits at the Ganmanong site (G in Figure 3b), would have been ~4830–4835 m elevation during MIS 5e. In terms of present-day elevations, because of the flexural rebound, our reconstructions suggest that any paleoshorelines developed around central Siling Co would, at present, be 45–65 m higher than equivalent paleoshorelines at Nam Co, depending on variations in the elastic thicknesses (Figure 3c).

The general pattern of flexural rebound driven by changes in surface loads requires that the shorelines near present-day Siling Co would have been deflected by greater amounts than those at Nam Co (Figure 2). In fact,

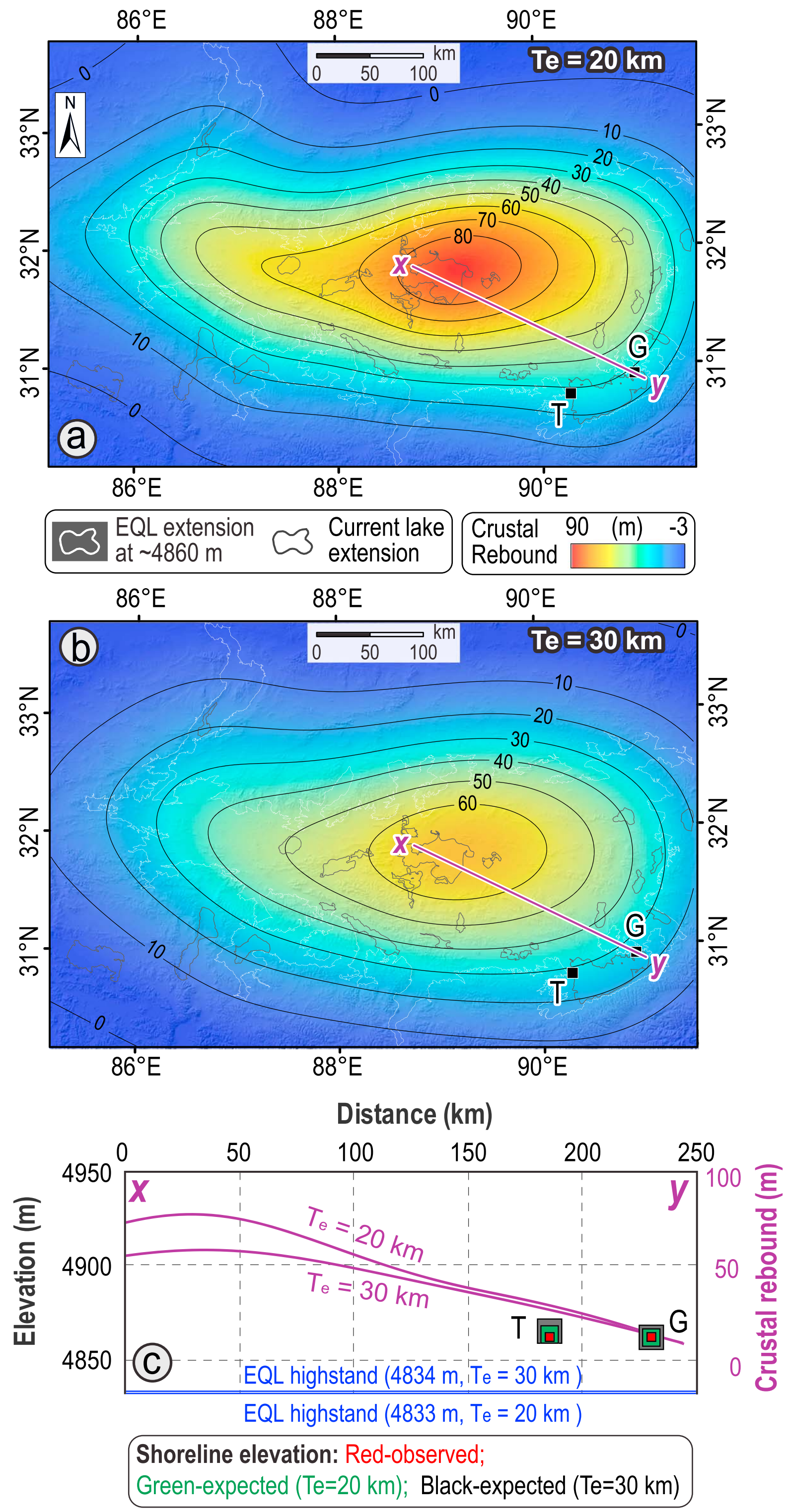

Figure 2. Calculation of expected shoreline elevations considering the crustal rebound induced by the lake unloading of the hypothesized East Qiangtang Lake (EQL). (a and b) The map pattern and contours (10 m interval) of the crustal rebound with crustal elastic thickness (T_e) of 20 km and 30 km [*Shi et al.*, 2015] for central Tibet, respectively. Numbers within the contours denote the magnitude of the rebound in meters. (c) The amount of crustal rebound along the profiles shown in Figures 2a and 2b. Also shown here is comparison of expected versus observed shoreline elevations at Ganmanong and Tajiguri sites around Nam Co.

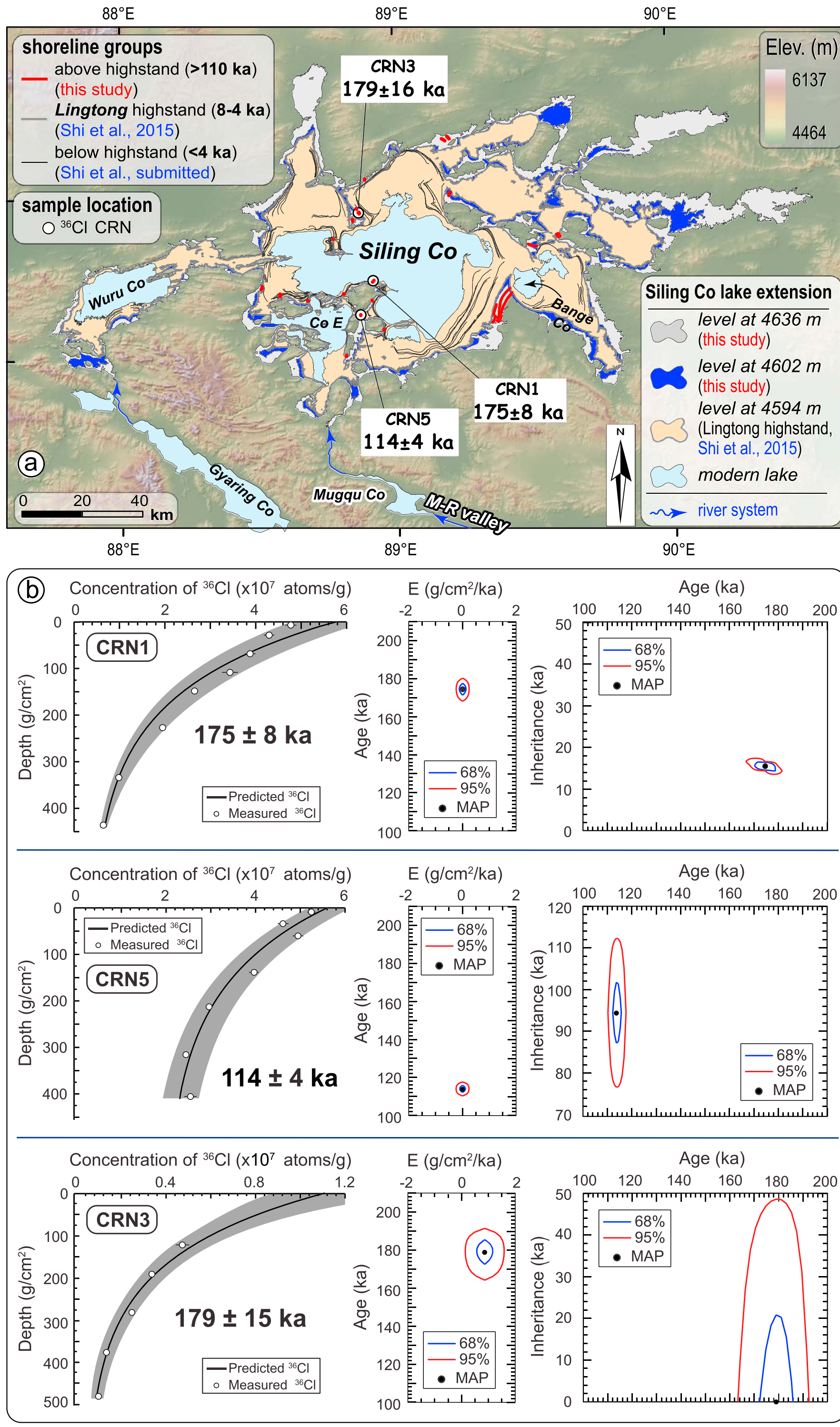

Figure 3. Geomorphology and chronology of highest shorelines around current Siling Co and paleolakes. (a) The map shows the lake extent of Siling Co at ~4636 m defined by the highest shorelines (red polygon), at ~4602 m (blue polygon), the Holocene Lingtong highstand (yellow polygon), and at modern time (light blue polygon). Also shown here are several groups of shorelines and sample locations and ages. (b) Cosmogenic ^{36}Cl depth profiles of CRN-1, CRN-3, and CRN-5. The solid curves represent model-predicted depth profile ^{36}Cl concentrations that best fit the measured concentrations. The gray shading shows the uncertainties of the depth profile concentrations with 95% confidence interval. The contour plots in each panel show the solutions from methodology of "maximum a posterior" (MAP) based on Bayesian inversion for ages, erosion rates, and inheritance of the shoreline deposits.

even if the elastic thickness were much greater than 20–30 km [*Shi et al*., 2015], reducing the magnitude of flexural rebound, the observed paleoshoreline elevations around Siling Co would still lie below predicted values. Although this result does not include the possibility of spatial variations in the rigidity of Tibetan lithosphere [e.g., *Chen et al*., 2015], unless such a variation was implausibly abrupt, we would expect a rebound pattern which to first order would be similar to that shown in Figure 2. We also do not consider the timescales associated with viscoelastic rebound, as this will not impact the final distribution of shoreline elevation. Finally, our result does not include any possible displacements along the active faults in the region [e.g., *Shi et al*., 2014; *Taylor et al*., 2003]. Of particular significance is the normal fault along the southeast side of the Nyainqentanglha Shan (Figure 1). Rebound of the footwall block of the east facing fault system may drive a west directed tilt that could influence the position of shorelines around Nam Co. Similarly, changes in the extent of alpine glaciers in the range itself could also be a local source of surface loading/unloading. However, we expect both of these possibilities to yield relatively small magnitude deflections, limited in their proximity to the Nyainqentanglha Shan. In fact, Holocene shorelines around Nam Co exhibit no variations in elevation that might be expected to result from local deflections [*England et al*., 2013; *Wallis et al*., 2010], and thus, we consider that to first order, our calculation of the expected lithospheric rebound is reasonable.

4.2. Age of High Shorelines at Siling Co

We dated paleoshorelines in the Siling Co basin to test the potential for correlation of shorelines around the EQL (Figure 1). Our modeling of paleoshoreline deflection suggests that former lake shorelines at this location would have experienced the greatest deflection from their initial elevations (Figure 2). Mapping of shoreline features shows that relict beach platforms and wave-cut shoreline scarps above the Holocene Lingtong highstand [*Shi et al*., 2015] are sporadically preserved around Siling Co (Figure 3a). Many of the best preserved, highest, paleoshoreline remnants are located in the area between Siling Co and Bange Co and atop the northern peninsula of Siling Co (Figure 3a). Notably, the highest paleoshorelines we observed around Siling Co are at 4636 m.

We collected three depth profiles of beach gravels (Figures 3a and S2a–S2c) from these highest shorelines and analyzed samples for cosmogenic ^{36}Cl exposure dating. One sample (CRN-5) was collected from a relict shoreline spit at 4596 m, immediately above the Holocene highstand shorelines (Figure 3 and Table S2), whereas the other two samples (CRN-1 and CRN-3) were collected from higher shorelines at 4601 m and 4636 m (the highest), respectively (Table S2). In general, all three depth profiles exhibit decreasing ^{36}Cl concentrations with depth that are reasonably described by an exponential, related to the attenuation of the secondary cosmic ray (fast nucleon) flux (Figure 3b). Profiles CRN-1 and CRN-5 yield very narrow bounds on both the age (within 10% at 2σ, Figure 3) and postdepositional erosion rate, consistent with our observations of intact preservation of the stratigraphy at the sites. Profile CRN-3, in contrast, has fewer samples near the top of the profile; this leads to larger uncertainties in surface erosion and therefore ^{36}Cl inheritance and deposit age. Overall, these sample concentrations appear to be consistent with a deposit with uniform inheritance that has remained relatively stable since deposition.

Modeling of the three depth profiles results in ages that range from 110 to 190 ka (Figure 3 and Table S2). The lowest elevation profile, CRN-5 (4596 m in elevation) has the youngest age of 114 ± 4 ka (Figure 3 and Table S2), suggesting that this tombolo formed during last interglacial time period, MIS 5e [*Lisiecki and Raymo*, 2005]. The other two samples, CRN-1 and CRN-3, have ages of 175 ± 8 ka and 179 ± 16 ka, respectively; both of these are within the MIS 6 glacial period, suggesting that Siling Co reached even greater extents (up to 4636 m, present elevation) during the glacial period.

Shorelines at similar elevations (~4590 m) have been previously dated at Bange Co (Figures 1 and 3), a small lake adjacent to Siling Co [*Zhao et al*., 2011]. Dating of carbonate material via U series yielded a ^{230}Th age of 167 ± 22 ka. The consistency of this result to our dating at the CRN-1 profile, at similar elevation (~4602 m, 175 ± 8 ka), suggests that the ages are reliable. Importantly, our results confirm that the highest shorelines at Siling Co formed during MIS6-5e, during the same time period as the hypothesized East Qiangtang Lake. In fact, the ^{36}Cl profile age of 114 ± 4 ka at the CRN-5 site (4596 m, Figure 3 and Table S3) is nearly the same as the U-Th age (116 ± 12 ka) of lacustrine deposits found at ~4860 m around Nam Co [*Zhu et al*., 2004]. This suggests that the shorelines in Siling Co and Nam Co formed contemporaneously, but at very different elevations.

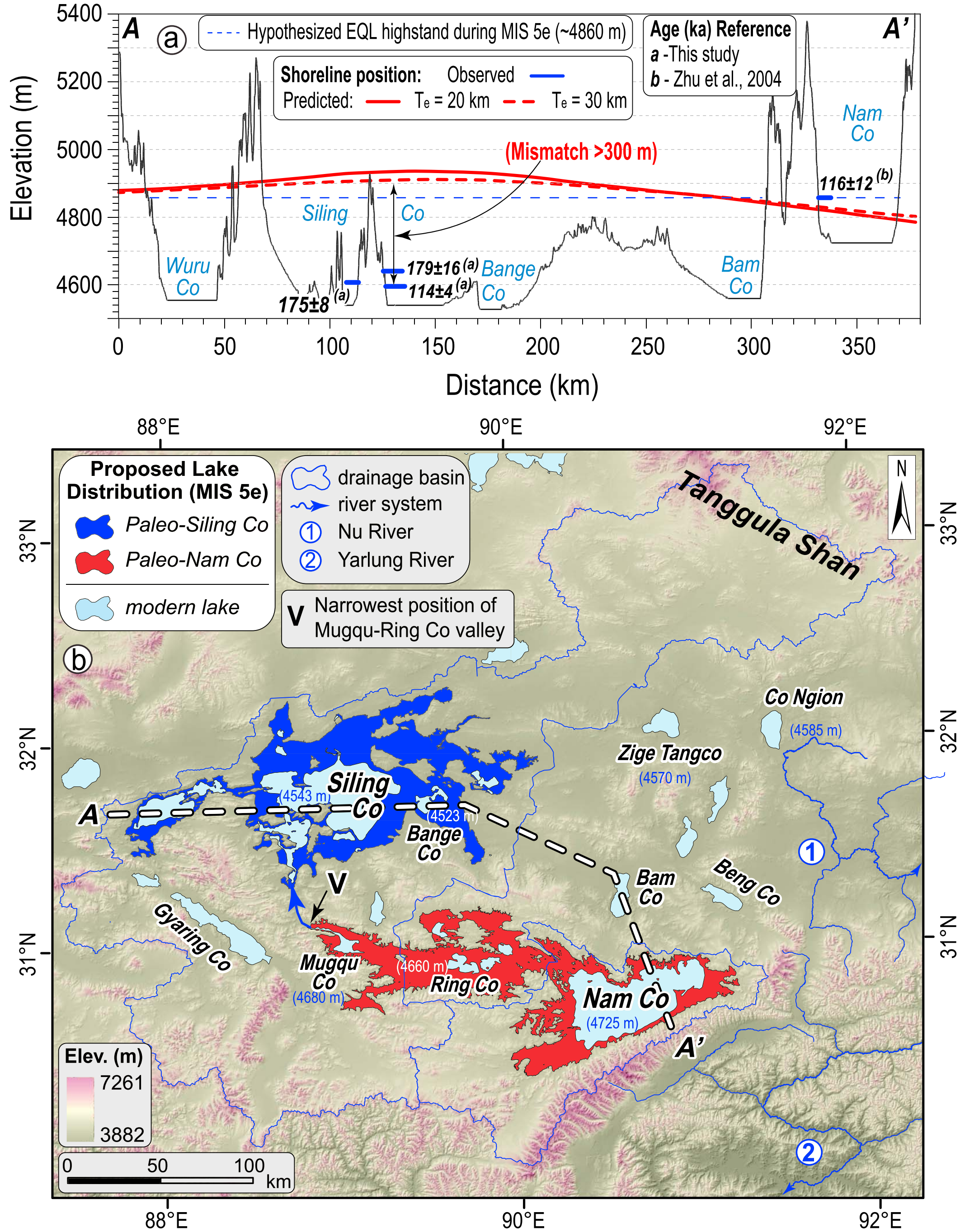

Figure 4. Lake distribution in central Tibet at modern time and during MIS 5e, proposed in this study. (a) Comparison between the predicted shoreline positions under the EQL hypothesis and observed shoreline elevations, relative to the EQL highstand at ~4860 m, along the topographic profile A-A′ (see location in Figure 4b). Also shown here is the chronologic correlation of shorelines and lacustrine deposits around Nam Co [*Zhu et al.*, 2004] and Siling Co (this study). Digital numbers show the sample ages (ka). (b) The spatial distribution, proposed in this study, of paleo-Siling Co at 4636 m elevation and paleo-Nam Co at ~4860 m elevation, during MIS 5e.

4.3. Implications for the East Qiangtang Lake Hypothesis

Our new observations and chronology from the highest shorelines around Siling Co are inconsistent with the model predictions of rebound of shorelines developed around a single large lake (Figure 4a). In terms of the present-day elevations, the flexural response of an elastic lithosphere to changes in water load predicts that MIS 5e shorelines around central Siling Co should sit 45–65 m higher than equivalent shorelines around Nam Co (Figure 2c). For example, the model predicts that shorelines at the CRN-5 site should presently lie at ~4920 m for T_e = 20 km or ~4900 m for T_e = 30 km. These predictions are greater than ~300 m above their present elevation (Figure 4a). Given that the chronology of both sets of shorelines suggests contemporaneous formation during MIS 5e, we conclude that any flexural rebound driven by changes in surface load would have to be much smaller in magnitude. That is, our results are difficult to reconcile with the hypothesis of a single, continuous lake in central Tibet during the late Pleistocene.

5. Discussion

Our study highlights the challenges of reconstructing paleoshorelines around ancient basins. The flexural response of the lithosphere to surface loads is a well-understood phenomenon [*Bills et al.*, 1994a, 2007, 1994b; *England et al.*, 2013; *Gilbert*, 1890; *Hampel and Hetzel*, 2006; *Shi et al.*, 2015], but it is not always applied when attempting to correlate geomorphic features. In the case of the EQL, previous research determined the height and extent of the lake based on the presence of shorelines at its very southeastern margin, near the present-day location of Nam Co. Both sites are approximately equidistant from the centroid of mass of the expected water load (Figure 2), and our flexural models demonstrate that they would be expected to have been deflected by similar amounts [*England et al.*, 2013; *Shi et al.*, 2016]. That is, they are expected to sit at similar elevations today (sites T and G, Figure 2). However, the greatest deflections and rebound are expected to occur near the center of the EQL, at the present-day location of Siling Co.

Our results from geomorphology, chronology, and deflections of the high paleoshorelines around Siling Co suggest that Siling Co and Nam Co were isolated lake basins during MIS 5e. The highest paleoshorelines with elevations around Siling Co between 4595 and 4636 m record the maximum extent of the paleo-Siling Co (color-coded polygons in Figure 4b). The extent of the paleo-Nam Co during MIS 5e (Figure 4b) appears to have been restricted to the Nam Co basin itself. It is possible that the lake extended to a farther western outlet ("V" in Figure 4b) in the narrow U-shaped Mugqu-Ring Co valley (Figure S4), but our results require that the lake did not extend to the Siling Co basin. Therefore, an alternative hypothesis for forming paleo-Nam Co at ~4860 m elevation is that the Nam Co drainage may have been dammed by temporary blockage, such as glacial moraines or a landslide, during the MIS 5e-6 periods.

The distribution of isolated, smaller lakes, instead of a single, unified giant lake within central Tibet, has important implications for the hydrologic balance and hence paleoclimate conditions during MIS 5e. Interestingly, the similarity of lake levels during MIS 5e (~4595 m), as indicated by the CRN-5 depth profile (Figures 3 and 4a), in the central peninsula to maximum lake levels during the early Holocene (Lingtong high-stand at ~4594 m) [*Shi et al.*, 2015]], suggests the possibility of similar extents of Siling Co during these two time periods (Figure 3a) and points to a potentially similar control on the lake level. Because the lake surface area is a determining factor in the water balance of the lake systems [e.g., *Benson and Paillet*, 1989], similar lake extents may simply suggest hydrologic balances during these two interglacial time periods. However, study of alternative explanations is also warranted.

6. Conclusions

Analysis of lithospheric flexure owing to the lake unloading and new shoreline data around Siling Co in central Tibet enables us to evaluate the size and extent of a hypothesized lake, proposed to occupy much of the central Tibetan Plateau during MIS 5e. Models of the flexural response of the lithosphere to these surface loads suggest that EQL shorelines at the lake center near present-day Siling Co are expected to be found 45–65 m higher than those around the lake margin near present-day Nam Co. However, new chronologic constraints of the highest paleoshorelines around Siling Co yield ages between 110 and 190 ka, indicating that they developed in MIS 6-5e, yet these relict shorelines are found more than 300 m lower than the EQL-expected, flexure-adjusted, elevations. Such a large discrepancy between the expected and observed shoreline elevations very likely invalidates the hypothesis of EQL in central Tibet during MIS 5e. Instead, our results suggest that Siling Co and Nam Co were local lake systems that were either isolated or connected by fluvial networks during MIS 5e.

Acknowledgments
This work was supported by a U.S. National Science Foundation grant (EAR-0911587) to E.K. and K.P.F. Additional support to E.W. was provided by grants from the Chinese Academy of Sciences (XDB03010500). X.S. also thanks the support from the Earth Observatory of Singapore (EOS), Nanyang Technological University through its funding from the National Research Foundation Singapore and the Singapore Ministry of Education under the Research Centers of Excellence initiative. We are grateful to Tashi Wangdi and Feng Qu for assistance of the field work. We thank two anonymous reviewers for providing constructive comments that improved the quality of this paper and thank Editor Kim Cobb for handling this paper. We declare no financial interests among the authors. Supporting data can be accessed in the supporting information file. This work comprises Earth Observatory of Singapore contribution 151.

References

Anderson, R. S., J. L. Repka, and G. S. Dick (1996), Explicit treatment of inheritance in dating depositional surfaces using in situ ^{10}Be and ^{26}Al, *Geology*, *24*(1), 47–51.

Aruscavage, P., and E. Campbell (1983), An ion-selective electrode method for determination of chlorine in geological materials, *Talanta*, *30*(10), 745–749.

Aumer, R. A. (2010), Calibration of low energy production of ^{36}Cl and the creation of an exposure age calculator, MS thesis, 48 pp., New Mexico Inst. of Mining and Tech., Socorro, N. M.

Avouac, J.-P., J.-F. Dobremez, and L. Bourjot (1996), Palaeoclimatic interpretation of a topographic profile across middle Holocene regressive shorelines of Longmu Co (western Tibet), *Palaeogeogr. Palaeoclimatol. Palaeoecol.*, *120*(1–2), 93–104.

Benson, L. V., and F. L. Paillet (1989), The use of total lake-surface area as an indicator of climatic change: Examples from the Lahontan basin, *Quat. Res.*, *32*(3), 262–275.

Bills, B. G., D. R. Currey, and G. A. Marshall (1994a), Viscosity estimates for the crust and upper mantle from patterns of lacustrine shoreline deformation in the eastern Great Basin, *J. Geophys. Res.*, *99*(B11), 22,059–22,086, doi:10.1029/94JB01192.

Bills, B. G., K. D. Adams, and S. G. Wesnousky (2007), Viscosity structure of the crust and upper mantle in western Nevada from isostatic rebound patterns of the late Pleistocene Lake Lahontan high shoreline, *J. Geophys. Res.*, *112*, B06405, doi:10.1029/2005JB003941.

Bills, B. G., S. L. de Silva, D. R. Currey, R. S. Emenger, K. D. Lillquist, A. Donnellan, and B. Worden (1994b), Hydro-isostatic deflection and tectonic tilting in the central Andes: Initial results of a GPS survey of Lake Minchin shorelines, *Geophys. Res. Lett.*, *21*(4), 293–296, doi:10.1029/93GL03544.

Blake, G. R., and K. H. Hartge (1986), Bulk density, in *Methods of Soil Analysis, Part I. Physical and Mineralogical Methods*, 2nd ed., edited by A. Klute, pp. 363–375, Agronomy Monography, Madison, Wisconsin.

Brotchie, J., and R. Silvester (1969), On crustal flexure, *J. Geophys. Res.*, *74*(22), 5240–5252, doi:10.1029/JB074i022p05240.

Chen, B., J. Liu, C. Chen, J. Du, and Y. Sun (2015), Elastic thickness of the Himalayan–Tibetan orogen estimated from the fan wavelet coherence method, and its implications for lithospheric structure, *Earth Planet. Sci. Lett.*, *409*, 1–14.

Dep, L., D. Elmore, J. Fabryka-Martin, J. Masarik, and R. C. Reedy (1994), Production rate systematics of in-situ-produced cosmogenic nuclides in terrestrial rocks: Monte Carlo approach of investigating ^{35}Cl (n, γ) ^{36}Cl, *Nucl. Instrum. Methods Phys. Res., Sect. B*, *92*(1–4), 321–325.

Desilets, D., M. Zreda, P. F. Almasi, and D. Elmore (2006), Determination of cosmogenic ^{36}Cl in rocks by isotope dilution: Innovations, validation and error propagation, *Chem. Geol.*, *233*(3–4), 185–195.

Dunne, J., D. Elmore, and P. Muzikar (1999), Scaling factors for the rates of production of cosmogenic nuclides for geometric shielding and attenuation at depth on sloped surfaces, *Geomorphology*, *27*(1–2), 3–11.

Elmore, D., and F. M. Phillips (1987), Accelerator mass spectrometry for measurement of long-lived radioisotopes, *Science*, *236*(4801), 543–550.

Elsheimer, H. N. (1987), Application of an ion-selective electrode method to the determination of chloride in 41 international geochemical reference materials, *Geostand. Newslett.*, *11*(1), 115–122.

England, P. C., R. T. Walker, B. Fu, and M. A. Floyd (2013), A bound on the viscosity of the Tibetan crust from the horizontality of palaeolake shorelines, *Earth Planet. Sci. Lett.*, *375*, 44–56.

Gasse, F., et al. (1991), A 13,000-year climate record from western Tibet, *Nature*, *353*(6346), 742–745.

Gilbert, G. (1890), *Lake Bonneville*, U.S. Geol. Surv., 438 pp., Washington, D. C.

Gosse, J. C., and F. M. Phillips (2001), Terrestrial in situ cosmogenic nuclides: Theory and application, *Quat. Sci. Rev.*, *20*(14), 1475–1560.

Hampel, A., and R. Hetzel (2006), Response of normal faults to glacial-interglacial fluctuations of ice and water masses on Earth's surface, *J. Geophys. Res.*, *111*, B06406, doi:10.1029/2005JB004124.

Hudson, A. M., and J. Quade (2013), Long-term east-west asymmetry in monsoon rainfall on the Tibetan Plateau, *Geology*, *41*(3), 351–354.

Hudson, A. M., J. Quade, T. E. Huth, G. Lei, H. Cheng, L. R. Edwards, J. W. Olsen, and H. Zhang (2015), Lake level reconstruction for 12.8–2.3 ka of the Ngangla Ring Tso closed-basin lake system, southwest Tibetan Plateau, *Quat. Res.*, *83*(1), 66–79.

Jordan, T. A., and A. B. Watts (2005), Gravity anomalies, flexure and the elastic thickness structure of the India–Eurasia collisional system, *Earth Planet. Sci. Lett.*, *236*(3–4), 732–750.

Kong, P., Y. Zheng, and B. Fu (2011), Cosmogenic nuclide burial ages and provenance of late Cenozoic deposits in the Sichuan Basin: Implications for early Quaternary glaciations in east Tibet, *Quat. Geochronol.*, *6*(3–4), 304–312.

Li, D., Y. Li, B. Ma, G. Dong, L. Wang, and J. Zhao (2009), Lake-level fluctuations since the last glaciation in Selin Co (lake), central Tibet, investigated using optically stimulated luminescence dating of beach ridges, *Environ. Res. Lett.*, *4*(045204), 1–10.

Lifton, N., T. Sato, and T. J. Dunai (2014), Scaling in situ cosmogenic nuclide production rates using analytical approximations to atmospheric cosmic-ray fluxes, *Earth Planet. Sci. Lett.*, *386*, 149–160.

Lisiecki, L. E., and M. E. Raymo (2005), A Pliocene-Pleistocene stack of 57 globally distributed benthic δ^{18}O records, *Paleoceanography*, *20*, PA1003, doi:10.1029/2004PA001071.

Marrero, S. (2009), Chlorine-36 Production Rate Calibration Using Shorelines from Pleistocene Lake Bonneville, Utah, MS thesis, 201 pp., New Mexico Inst. of Mining and Tech., Socorro, N. M.

Marrero, S. (2012), Calibration of Cosmogenic Chlorine-36, PhD thesis, 365 pp., New Mexico Inst. of Mining and Tech., Socorro, N. M.

Marrero, S. M., F. M. Phillips, M. W. Caffee, and J. C. Gosse (2016a), CRONUS-Earth cosmogenic ^{36}Cl calibration, *Quat. Geochronol.*, *31*, 199–219.

Marrero, S. M., F. M. Phillips, B. Borchers, N. Lifton, R. Aumer, and G. Balco (2016b), Cosmogenic nuclide systematics and the CRONUScalc program, *Quat. Geochronol.*, *31*, 160–187.

Meng, K., X. Shi, E. Wang, and F. Liu (2012a), High-altitude salt lake elevation changes and glacial ablation in central Tibet, 2000–2010, *Chin. Sci. Bull.*, *57*(5), 525–534.

Meng, K., X. Shi, E. Wang, and Z. Su (2012b), Geomorphic characteristics, spatial distribution of paleoshorelines around the Siling Co area, central Tibet, and the lake evolution within the plateau [in Chinese with English abstract], *Chin. J. Geol.*, *47*(3), 730–745.

Muzikar, P., D. Elmore, and D. E. Granger (2003), Accelerator mass spectrometry in geologic research, *Geol. Soc. Am. Bull.*, *115*(6), 643–654.

Nakiboglu, S. M., and K. Lambeck (1983), A reevaluation of the isostatic rebound of Lake Bonneville, *J. Geophys. Res.*, *88*(B12), 10,439–10,447, doi:10.1029/JB088iB12p10439.

Phillips, F. M., J. P. Ayarbe, J. B. J. Harrison, and D. Elmore (2003), Dating rupture events on alluvial fault scarps using cosmogenic nuclides and scarp morphology, *Earth Planet. Sci. Lett.*, *215*(1–2), 203–218.

Rades, E. F., S. Tsukamoto, M. Frechen, Q. Xu, and L. Ding (2015), A lake-level chronology based on feldspar luminescence dating of beach ridges at Tangra Yum Co (southern Tibet), *Quat. Res.*, *83*, 469–478.

Schimmelpfennig, I., L. Benedetti, R. Finkel, R. Pik, P.-H. Blard, D. Bourlès, P. Burnard, and A. Williams (2009), Sources of in-situ ^{36}Cl in basaltic rocks. Implications for calibration of production rates, *Quat. Geochronol.*, *4*(6), 441–461.

Shao, Z., X. G. Meng, J. E. Han, D. Zhu, C. Yang, J. Wang, J. Yu, Y. Wang, and C. He (2013), Definition of the Quaternary Qiangtang Paleolake in Qinghai-Tibetan Plateau, China, *Acta Geol. Sin.*, *87*(2), 607–617.

Shi, X., E. Kirby, and K. P. Furlong (2016), Reply to comment on "crustal strength in central Tibet determined from Holocene shoreline deflection around Siling Co", *Earth Planet. Sci. Lett.*, *433*, 396–398.

Shi, X., E. Kirby, H. Lu, R. Robinson, K. P. Furlong, and E. Wang (2014), Holocene slip rate along the Gyaring Co fault, central Tibet, *Geophys. Res. Lett.*, *41*, 5829–5837, doi:10.1002/2014GL060782.

Shi, X., E. Kirby, K. P. Furlong, K. Meng, R. Robinson, and E. Wang (2015), Crustal strength in central Tibet determined from Holocene shoreline deflection around Siling Co, *Earth Planet. Sci. Lett.*, *423*, 145–154.

Stone, J. O., G. L. Allan, L. K. Fifield, and R. G. Cresswell (1996), Cosmogenic chlorine-36 from calcium spallation, *Geochim. Cosmochim. Acta*, *60*(4), 679–692.

Taylor, M., A. Yin, F. J. Ryerson, P. Kapp, and L. Ding (2003), Conjugate strike-slip faulting along the Bangong-Nujiang suture zone accommodates coeval east-west extension and north-south shortening in the interior of the Tibetan Plateau, *Tectonics*, *22*(4), 1044, doi:10.1029/2002TC001361.

Wallis, S. R., H. Mori, K. Ozawa, M. Mitsuishi, and C. Shirakawa (2010), Lake shoreline deformation in Tibet and mid-crustal flow, *Island Arc*, *19*, 209–211.

Watts, A. B. (2001), *Isostasy and Flexure of the Lithosphere*, 458 pp., Cambridge Univ. Press, Cambridge.

Wei, Z., R. Huang, W. Chen, and W. Dong (2002), Spatial distributions and interdecadal variations of the snow at the Tibetan Plateau weather stations [in Chinese with English abstract], *Chin. J. Atmos. Sci.*, *26*(4), 496–508.

Yang, M., T. Yao, F. Nelson, N. Shiklomanov, D. Guo, and C. Wang (2008), Snow cover and depth of freeze-thaw on the Tibetan Plateau: A case study from 1997 to 1998, *Phys. Geogr.*, *29*(3), 208–221.

Zhang, G., H. Xie, S. Kang, D. Yi, and S. F. Ackley (2011a), Monitoring lake level changes on the Tibetan Plateau using ICESat altimetry data (2003–2009), *Remote Sens. Environ.*, *115*(7), 1733–1742.

Zhang, G., H. Xie, S. Duan, M. Tian, and D. Yi (2011b), Water level variation of Lake Qinghai from satellite and in situ measurements under climate change, *J. Appl. Remote. Sens.*, *5*(1), 053532–053532.

Zhang, G., T. Yao, H. Xie, K. Zhang, and F. Zhu (2014), Lakes' state and abundance across the Tibetan Plateau, *Chin. Sci. Bull.*, *1-12*.

Zhao, X., Y. Zhao, M. Zheng, Z. Ma, J. Cao, and M. Li (2011), Late Quaternary lake development and genivellation of Bankog Co as well as lake evolution of southeastern north Tibetan Plateau during the last great lake period [in Chinese with English abstract], *Acta Geosci. Sin.*, *32*(1), 13–26.

Zhu, D., X. Meng, X. Zhao, Z. Shao, Z. Xu, C. Yang, Z. Ma, Z. Wu, Z. Wu, and J. Wang (2004), Evolution of an ancient large lake in the southeast of the northern Tibetan Plateau, *Acta Geol. Sin.*, *78*(4), 982–992.

Zhu, D., X. Zhao, X. Meng, Z. Wu, Z. Wu, X. Feng, Z. Shao, Q. Liu, and M. Yang (2002), Quaternary lake deposits of Nam Co, Tibet, with a discussion of the connection of Nam Co with Ring Co-Jiuru Co, *Acta Geol. Sin.*, *76*(3), 283–291.